Miroslav Trcala; Ivan Němec; Adéla Vaněčková; Filip Hokeš
Dynamic analysis of viscous material models

In: Jan Chleboun and Pavel Kůs and Petr Přikryl and Miroslav Rozložník and Karel Segeth and Jakub Šístek (eds.): Programs and Algorithms of Numerical Mathematics, Proceedings of Seminar. Hejnice, June 21-26, 2020. Institute of Mathematics CAS, Prague, 2021. pp. 139–148.

Persistent URL: http://dml.cz/dmlcz/703109

Programs and Algorithms of Numerical Mathematics 20
J. Chleboun, P. Kůs, P. Přikryl, M. Rozložník, K. Segeth, J. Šístek (Eds.)
Institute of Mathematics of the Czech Academy of Sciences, Prague 2021

DYNAMIC ANALYSIS OF VISCOUS MATERIAL MODELS

Miroslav Trcala, Ivan Němec, Adéla Vaněčková, Filip Hokeš

Brno University of Technology, Faculty of Civil Engineering,
Institute of Structural Mechanics,
602 00 Brno, Veveří 331/95, Czech Republic
trcala@fem.cz, nemec@fem.cz, vaneckova@fem.cz, hokes@fem.cz

Abstract: The article deals with the analysis of the dynamic behavior of a concrete structural element during fast dynamic processes. The constitutive material model must be chosen appropriately so that it takes material viscosity into account when describing the behavior of material. In this analysis, it is necessary to use fairly complex viscous material models which can affect, for example, vibration damping and the dependence of strength or even of the entire stress-strain curve on the strain rate. These relatively complex models are often formed via the combination of viscoelastic models with viscoplastic models or viscous damage models. Numerical simulations are performed for these models. The numerical analysis is validated by experimental measurements.

Keywords: dynamic damping, Rayleigh damping, material viscosity

MSC: 74H05, 74H45, 74C10

1. Introduction

Within the field of engineering, research of constitutive relations is of key importance in the effort to ensure numerical simulations to correctly express the mechanical characteristics of concrete under complex loading conditions. Many tests have already proved that concrete has typical mechanical properties, such as the demonstration of different mechanical characteristics under uniaxial tensile and compressive loading conditions, stiffness degradation under cyclic loading conditions, irreversible deformations after unloading, unilateral and rate-dependent effects, etc. Inelastic deformation can be simulated by the plastic theory (see [5]), while, e.g., stiffness degradation and the unilateral effect can be researched through the damage theory (see [6]). In recent years, many researchers have combined the two theories together to form a coupled elastic-plastic damage model (see [7], [8], [9]). The strength of concrete increases with increasing strain rate. Strain rates in the 1 to 10 per second (-/sec) range will produce peak strength increases of about 20 to 50 percent in

DOI: 10.21136/panm.2020.14

compression and notably more than 100 percent in tension (see [1], [2]). The initial elastic modulus does not change significantly with strain rate, but its change is important for the vibration damping of concrete structures (see [4]).

2. Theory

2.1. The visco-elastic-visco-plastic-damage material model

This combined model is based on several sub-models: *a) viscoelastic model, b) viscoplastic model* and *c) viscodamage model*. The first of the above-mentioned models uses the Standard Linear Solid (SLS) (see [4]) model for the calculation of viscoelastic response. The second model in the resultant combination takes into account plasticity with viscosity (strain rate effect) via Dynamic Increase Factor (d_f) curves and its output is the viscoplastic response. The last model in the combination takes damage with viscosity into account again via d_f curves, but in this case the output is the viscodamage response. The resulting constitutive relationship for the described final combination is as follows:

$$\sigma = (\mathbf{I} - \mathbf{D}) : \mathbf{C} : (\varepsilon - \varepsilon^{ve} - \varepsilon^{vp}) \,, \tag{1}$$

where $\mathbf{I}$ is the fourth-order identity tensor, $\mathbf{D}$ is the fourth-order damage tensor, $\mathbf{C}$ is the fourth-order elasticity tensor, ε is the second-order strain tensor, ε^{ve} is the second-order visco-elastic part of strain tensor, ε^{vp} is the second-order viscoplastic part of the strain tensor. The following viscoelastic prediction and viscoplastic/damage correction were implemented (it is a common iteration process in material nonlinearity):
1) *Viscoelastic prediction*, based on the theory of visco-elasticity (Standard Linear Solid model) (see [4]). The material model inputs are a) the strain tensor reduced by viscoplastic ε_n^{vp} and viscodamage ε_n^{vd} strain tensors from the previous increment ε_{n+1} - ε_n^{vp} - ε_n^{vd} and b) all the state variables from the previous increment for the viscoelastic model. The output is the viscoelastic strain in the current increment ε_{n+1}^{ve}. It applies $\varepsilon_{n+1} = \varepsilon_{n+1}^{e1} + \varepsilon_{n+1}^{ve} + \varepsilon_n^{vp} + \varepsilon_n^{vd}$ and $\sigma_{n+1}^1 = \mathbf{C} : \varepsilon_{n+1}^{e1}$, where ε_{n+1}^{e1} is the first estimate of the elastic strain tensor and σ_{n+1}^1 is the corresponding first estimate of the stress tensor.
2) *Viscoplastic correction*, based on the theory of plasticity (Rankine-Hill model) (see [5]) with viscosity according to d_f curve. The material model inputs are a) the strain tensor reduced with the current viscoelastic strain tensor ε_{n+1}^{ve} and the viscoplastic/damage strain tensors ε_n^{vp}, ε_n^{vd} from the previous increment $\varepsilon_{n+1} - \varepsilon_{n+1}^{ve} - \varepsilon_n^{vp} - \varepsilon_n^{vd}$ and b) all the state variables from the previous increment for the viscoplastic model including for example the accumulated viscoplastic strain and so on. The output is the viscoplastic strain in the current increment ε_{n+1}^{vp}. It applies $\varepsilon_{n+1} = \varepsilon_{n+1}^{e2} + \varepsilon_{n+1}^{ve} + \varepsilon_{n+1}^{vp} + \varepsilon_n^{vd}$ and $\sigma_{n+1}^2 = \mathbf{C} : \varepsilon_{n+1}^{e2}$, where ε_{n+1}^{e2} is the second estimate of the elastic strain tensor and σ_{n+1}^2 is the corresponding second estimate of the stress tensor.
3) *Viscodamage correction*, based on the damage theory (Mazars model) (see [6]) with viscosity according to the d_f curve. The material model inputs are a) $\varepsilon_{n+1} -$

$\varepsilon_{n+1}^{ve} - \varepsilon_{n+1}^{vp} - \varepsilon_{n+1}^{vd}$ and b) all the state variables from the previous increment for the viscodamage model including for example damage parameters and also accumulated plastic strains in tension and compression. The output is the viscodamage strain ε_{n+1}^{vd}, the viscodamage in tension d_{n+1}^{vt}, the viscodamage in compression d_{n+1}^{vc} in the current increment. It applies $\varepsilon_{n+1} = \varepsilon_{n+1}^{e3} + \varepsilon_{n+1}^{ve} + \varepsilon_{n+1}^{vp} + \varepsilon_{n+1}^{vd}$ and $\sigma_{n+1}^{3} = \mathbf{C} : \varepsilon_{n+1}^{e3}$, where ε_{n+1}^{e3} is the third estimate of the elastic strain tensor and σ_{n+1}^{3} is the corresponding third estimate of the stress tensor. Then the resulting stress tensor is equal to:

$$\sigma_{n+1} = \sigma_{n+1}^{3} = \mathbf{C} : \varepsilon_{n+1}^{e3} = \mathbf{C} : (\varepsilon_{n+1} - \varepsilon_{n+1}^{ve} - \varepsilon_{n+1}^{vp} - \varepsilon_{n+1}^{vd}). \tag{2}$$

This is consistent with the above mentioned constitutive relationship (1), the damage tensor $\mathbf{D}_{n+1}$ derived from the resulting damage parameters corresponds to the resulting viscodamage strain tensor ε_{n+1}^{vd}. Both equations ((1) and (2)) yield the same resulting stress tensor σ_{n+1} which is the most important result because the internal nodal forces in the finite element method are calculated from this quantity and it is used in the Newton-Raphson method.

2.2. Damping

To estimate the approximate material parameters of the *Standard Linear Solid* (SLS) the equation of motion with damping (see (3)) was applied. For the SLS model, two unknown parameters had to be set so that the oscillation was damped by a relative damping of 2–3% according to the standard. The unknown parameters were approximately quantified by inverse analysis. The values of the parameters were determined from a single degree of freedom task (1D element with one node fixed and with zero initial condition).

$$\ddot{u} + 2\xi\omega_n\dot{u} + \omega_n^2 u = \left(\frac{\omega_n^2}{k}\right) p\,(t) \tag{3}$$

$$\xi = \frac{c}{c_{cr}}, \quad \omega_n = \sqrt{\frac{k}{m}} \tag{4}$$

where u is displacement, k is stiffness, m is mass, $p(t)$ is loading, ξ is relative damping, c is actual damping, c_{cr} is critical damping.

2.3. Dynamic Increase Factor

Viscous behavior in the visco-plasticity/damage combination was taken into account using the *Dynamic Increase Factor* (d_f) concept. This factor is defined as the ratio of the dynamic and static strength of concrete in relation to the strain rate. As far as the prepared software tool for the Dlubal RFEM computer program is concerned, a specific method was chosen for determining d_f according to the international recommendations stated in the document *CEB Model Code* (CEB-FIP

Model Code 1990) [3]. For the calculation of d_f it is needed to calculate the effective strain rate $\dot{\varepsilon}_{ef}$, i.e.,

$$\dot{\varepsilon}_{ef} = \sqrt{\frac{2}{3}\{(\dot{\varepsilon}_x - \dot{\varepsilon}_y)^2 + (\dot{\varepsilon}_x - \dot{\varepsilon}_z)^2 + (\dot{\varepsilon}_z - \dot{\varepsilon}_y)^2 + \dot{\varepsilon}_{xy}^2 + \dot{\varepsilon}_{xz}^2 + \dot{\varepsilon}_{yz}^2\}}. \tag{5}$$

2.3.1. Dynamic Increase Factor for compressive loading

According to the CEB model, in the tensile area the calculation of the d_f must be divided into two intervals depending on the strain rate:

$$\text{a)} \quad \text{For } \dot{\varepsilon}_{ef} \leq 30\, s^{-1}\text{: } d_f = \frac{f_c}{f_{cs}} = \left(\frac{\dot{\varepsilon}_{ef}}{\dot{\varepsilon}_s}\right)^{1{,}026\alpha_s} \tag{6}$$

$$\text{b)} \quad \text{For } \dot{\varepsilon}_{ef} > 30\, s^{-1}\text{: } d_f = \frac{f_c}{f_{cs}} = \gamma_s \left(\frac{\dot{\varepsilon}_{ef}}{\dot{\varepsilon}_s}\right)^{\frac{1}{3}}, \tag{7}$$

where d_f is the Dynamic Increase Factor, f_c and f_{cs} is the dynamic compressive strength at the strain rate $\dot{\varepsilon}_{ef}$, or the static strength at the strain rate $\dot{\varepsilon}_{ef}$. The validity of the relations above lies in the range $[30 \cdot 10^{-6}; 300]$ s^{-1} for the strain rate $\dot{\varepsilon}_{ef}$, and the static level of strain $\dot{\varepsilon}_s$ is considered to be $30 \cdot 10^{-6}$ s^{-1}. It is true for the coefficient γ_s that

$$\log \gamma_s = 6.15\alpha_s - 2, \quad \text{where } \alpha_s = \frac{1}{5 + 9\frac{f_{cs}}{f_{co}}} \tag{8}$$

in which the value f_{co} is considered to be $10\, MPa$. The relations above show that the d_f is higher for concretes with lower compressive strength.

2.3.2. Dynamic Increase Factor for tensile loading

The relation for the calculation of the d_f factor in tension depending on the size of the strain rate is defined by the relations:

$$\text{a)} \quad \text{For } \dot{\varepsilon}_{ef} \leq 30\, s^{-1}\text{: } d_f = \frac{f_t}{f_{ts}} = \left(\frac{\dot{\varepsilon}_{ef}}{\dot{\varepsilon}_s}\right)^{1{,}016\delta} \tag{9}$$

$$\text{b)} \quad \text{For } \dot{\varepsilon}_{ef} > 30\, s^{-1}\text{: } d_f = \frac{f_t}{f_{ts}} = \beta \left(\frac{\dot{\varepsilon}_{ef}}{\dot{\varepsilon}_s}\right)^{\frac{1}{3}} \tag{10}$$

where d_f is Dynamic Increase Factor, f_t and f_{ts} is the dynamic tensile strength at the strain rate $\dot{\varepsilon}_{ef}$, or the static strength at the strain rate $\dot{\varepsilon}_{ef}$. The validity of the above relations lies in the range $[30 \cdot 10^{-6}; 300]$ s^{-1} for the strain rate $\dot{\varepsilon}_{ef}$, and the static level of strain rate $\dot{\varepsilon}_s$ is considered to be $30 \cdot 10^{-6}$ s^{-1}. It is true for the coefficient β that

$$\log \beta = 7.11\delta - 2.33, \quad \text{where } \delta = \frac{1}{10 + 6\frac{f_{ts}}{f_{co}}} \tag{11}$$

in which the value f_{co} is considered to be 10 MPa. It follows from the relations above that the d_f is higher for concretes with lower tensile strength and contains a discontinuity at the strain rate of 30 s^{-1}.

3. Benchmark and experiment

The first basic validation of the material model was done using the benchmark model (Figure 1). The benchmark model was based on a single 3D solid finite element which was loaded in tension and compression by controlled deformation. The one dimensional stress state was ensured by a suitable boundary condition. The results are calculated for different strain rates.

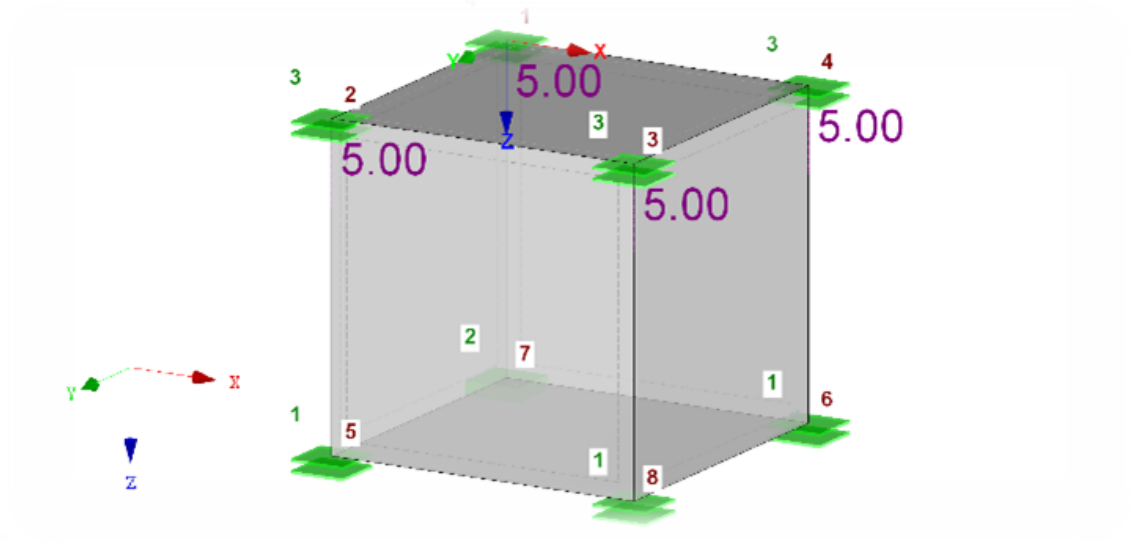

Figure 1: Benchmark model.

The main validation simulations were performed on a computational model of a reinforced concrete beam which was used in laboratory tests. The experiment involved measuring the dynamic response of a beam exposed to the impact of a punch in a drop weight tester. The beam (dimensions $1.7 \times 0.25 \times 0.12$ m) was placed simply on wooden supports and subjected to impact of a falling 500 kg weight.

Based on the real shape of the reinforced concrete beam, an idealized 2D computational model (see the Figure 2)was created from planar elements in the Dlubal RFEM system environment, which enables dynamic analyses in nonlinear dynamics. The simplification of the investigated process into a planar model was performed in order to reduce the computational time. As part of the idealization of the computational model, the employed wooden supports were modeled as flexible line supports with pressure only supports with corresponding stiffness. Using this support nonlinearity, the real upward jerking of the beam after contact with the punch could

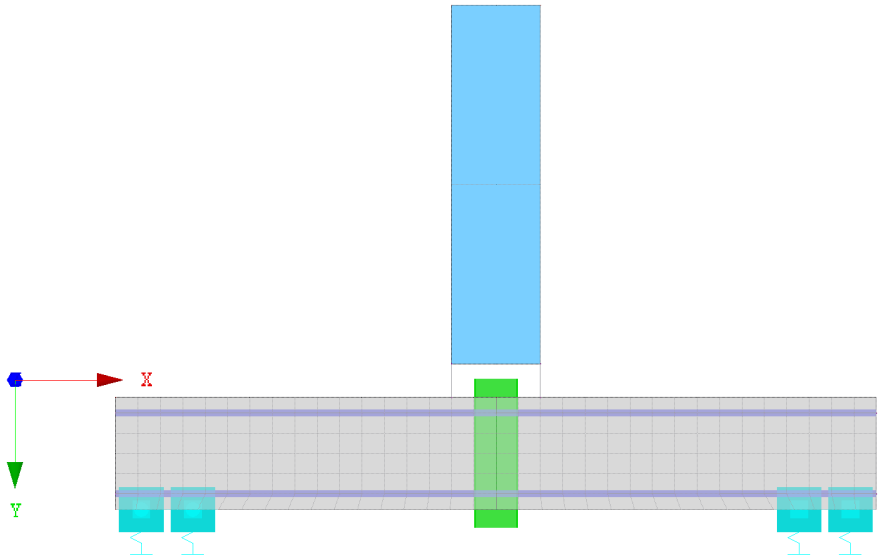

Figure 2: Model of the reinforced concrete beam in software RFEM.

be simulated. To validate the input quantities, the response of the beam to the fall of a weight from the height of 75 cm was measured during the experimental research. The numerical simulation was modeled as a contact of two bodies. An explicit method for solving equations of motion was used for the calculations.

In order to compare the material model with the experimental measurements, the deflection at mid-beam on its upper line at the point of impact of the punch was measured with a camera. We tested three d_f curves (d_f^1, d_f^2, d_f^3). The d_f^2 curve represented the concrete class 22 MPa and it was calculated according to the $CEB\ Model\ Code$ (CEB-FIP Model Code 1990)[3] (equation (6)–(11)). The d_f^1 curve was lower than d_f^2 curve and d_f^3 curve was higher than d_f^2 curve. Next we tested three variants of the SLS model (SLS1, SLS2, SLS3) with the respective viscosities $1.2e^7$, $1.2e^8$ (the closest to the experiment), $1.2e^9$.

4. Numerical results

4.1. Verification the Dynamic Increase Factor of the effect

For the material model a single-element verification study was performed first. The results show the ability of the model to respond correctly to different strain rates (see the figures 3 and 4 below). The numerical results obtained from the FEM model were exactly the same as the results obtained from the analytical equations ((5)–(11)).

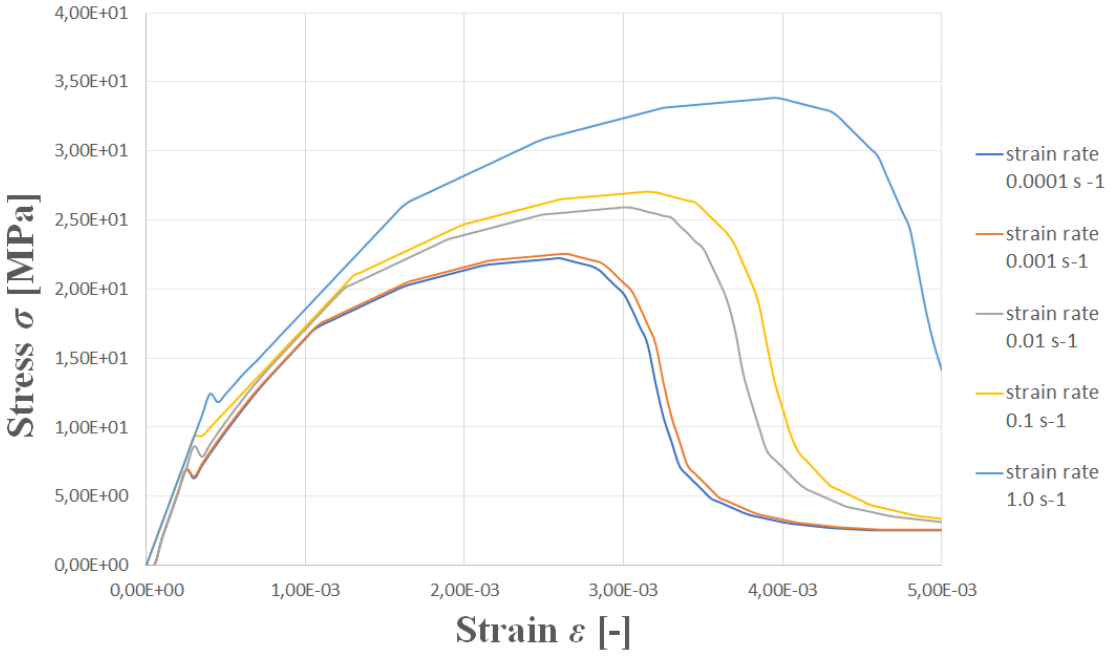

Figure 3: Influence of the strain rate effect on uniaxial compressive stress-strain curve.

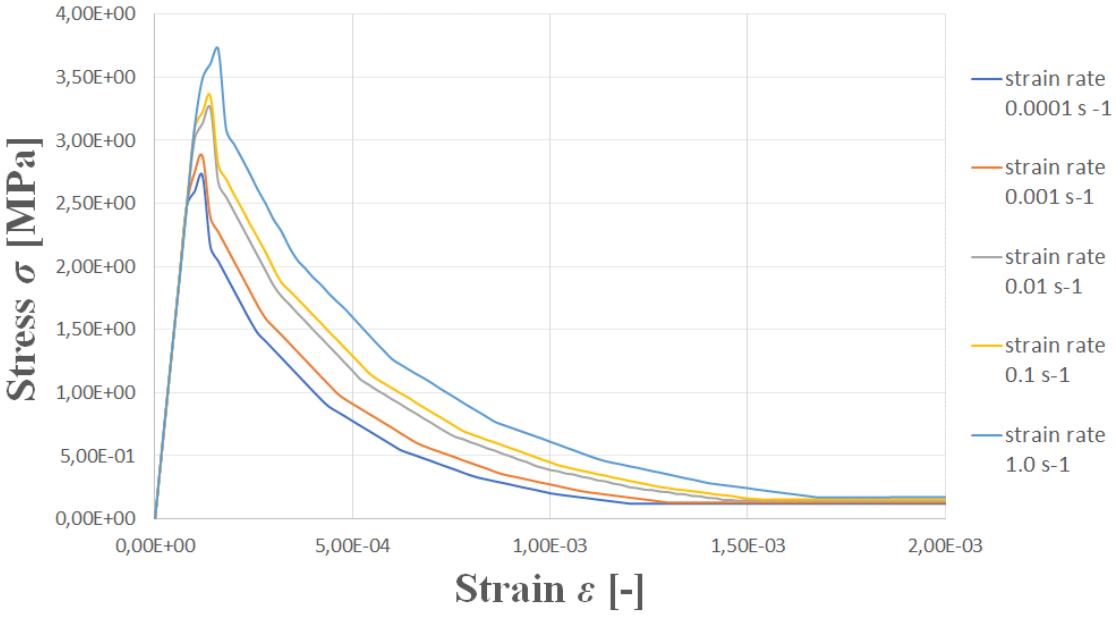

Figure 4: Influence of the strain rate effect on uniaxial tensile stress-strain curve.

4.2. Dynamic response of a reinforced concrete beam to the impact in a drop test device

The graphs (see the Figures 5, 6 below) show the effects of two different factors on the dynamic response of a reinforced concrete beam: 1) the influence of the viscoelastic model; 2) the influence of the dynamic increase factor. Each graph shows time curves of the experimentally measured and numerically calculated vertical deformation (deflection – displacement in the vertical direction) at the middle of the upper side of the beam. The best of all the calculated variants was the combination of $d_f 2$ curve with SLS2 (for damped oscillations $2-3\%$) because the results were the closest to those from the experimental measurements (see the Figures 5 and 6 below).

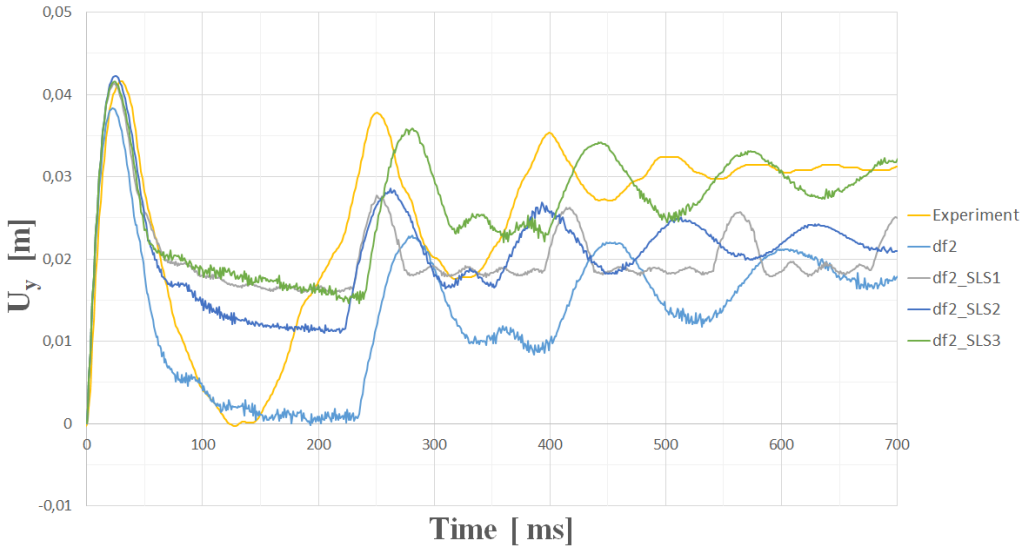

Figure 5: Influence of the visco-elastic model.

Conclusion

The use of a visco-elasto-visco-plastic-damage constitutive model to investigate the behavior of concrete under dynamic loading is presented. The plasticity is established in effective stress space with the Rankine-Hill criterion, while the damage part is based on equivalent strains in tension and compression. Viscous regularization of the elasto-plastic-damage model is implemented to include the rate effects, including the d_f curves and damping. The correct use of the rate effect is validated by the benchmark. Further, the presented material model is used for modeling the above described experiment with various input parameters with aim to find the parameters, which fit experiment as well as possible. The best results are obtained when using the following parameters: 1) SLS2 parameters which are determined so as to dampen

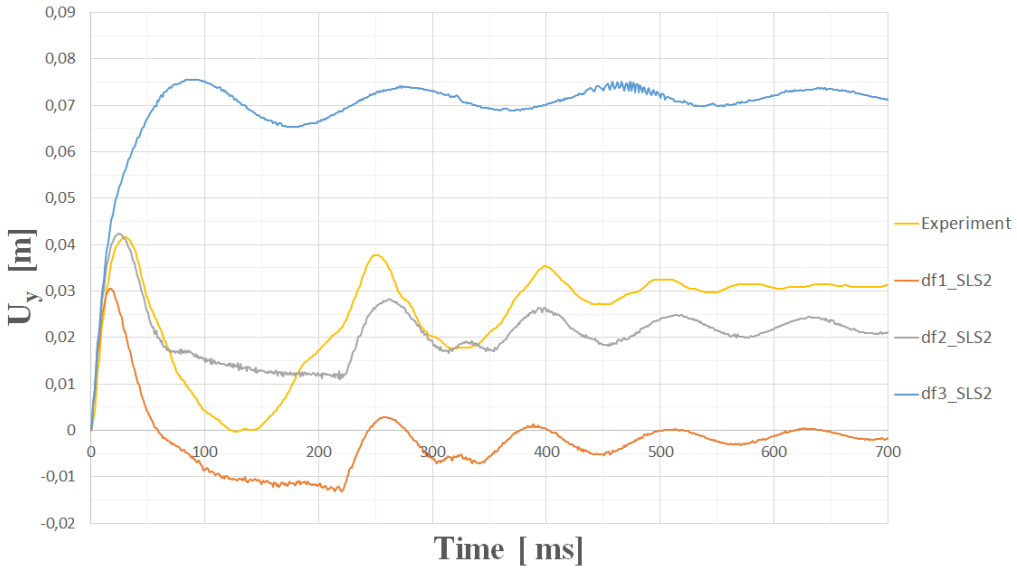

Figure 6: Influence of the dynamic increase factor.

the oscillations by a relative damping of $2-3\%$ according to the standard, 2) $d_f 2$ parameters corresponding to the concrete class used in the experiment ($22\ MPa$). The values of the parameters are determined by comparison of the numerical results with the experiment and the best agreement is achieved for these parameters. It can be concluded that the presented model can effectively simulate the mechanical behavior of concrete under dynamic loading.

Acknowledgement

This project was implemented with financial support from the Czech state budget via the Ministry of Industry and Trade within the program TRIO FV20372 Software tool for nonlinear analysis of concrete structures under fast dynamic processes.

References

[1] Bischoff, P. H., Perry, S. H.: *Impact behavior of plain concrete loaded in uniaxial compression.* J. Eng. Mech. (1995), 501–516.

[2] Malvar, L. J., and Ross, C. A.: *Review of static and dynamic properties of concrete in tension.* ACI Materials Journal. December (1998).

[3] Comité Euro-International du Béton: *CEB-FIP Model Code 1990.* Comité Euro-International du Béton, Thomas Telford House, 1993.

[4] Němec, I., Trcala, M., Vaněčková, A., and Rek, V.: *Dynamic damping - comparison of different concepts from the ponit of view of their physical nature and effects on civil engineering structures*. In: Chleboun, J., Kůs, P., Přikryl, P., Rozložník, M., Segeth, K., Šístek, J., and Vejchodský, T. (eds.): Programs and Algorithms of Numerical Mathematics, Proceedings and numerical Mathematics, Proceedings of Seminar, Hejnice, June 24–29, 2018. Institute of Mathematics CAS, pp. 107–118. Prague, 2019.

[5] Lourenco, P. B., de Borst, R., and Rots, J. G.: *A plane stress softening plasticity model for orthotropic materials*. Int. J. Numer. Meth. Engng. **40** (1997), 4033–4057.

[6] Mazars, J., Hamon, F., and Grange, S.: *A new 3D damage model for concrete under monotonic, cyclic and dynamic loadings*. Mater Struct. **48** (2015), 3779–3793.

[7] Wu, J. Y., Li, J., and Faria, R.: *An energy release rate-based plastic-damage model for concrete*. Int. J. Solids Struct. **43** (2006), 583–612.

[8] Lee, J., and Fenves, GL.: *Plastic-damage model for cyclic loading of concrete structures*. J. Eng. Mech.: ASCE 1998. **124** (1998), 892–900.

[9] Wu, J. Y., Li, J., and Faria, R.: *Unified plastic-damage model for concrete and its applications to dynamic nonlinear analysis of structures*. Struct. Eng. Mech. **25** (2007), 519–540.